A Tripod Molecular Tip for Single Molecule Ligand–Receptor Force Spectroscopy by AFM

ARTICLE *in* LANGMUIR · DECEMBER 2009

Impact Factor: 4.46 · DOI: 10.1021/la904151h · Source: PubMed

Langmuir
Article
pubs.acs.org/Langmuir

A Tripod Molecular Tip for Single Molecule Ligand−Receptor Force Spectroscopy by AFM

Michael E. Drew,[†] Arkadiusz Chworos,[‡] Emin Oroudjev,[‡] Helen Hansma,[‡] and Yoko Yamakoshi*[,†,§]

[†]*Department of Chemistry, and* [§]*Department of Radiology, University of Pennsylvania, 231 South 34th Street, Philadelphia Pennsylvania 19104-6323, and* [‡]*Department of Physics, University of California at Santa Barbara, Santa Barbara, California 93106-9530*

Received November 1, 2009

Tripod-shaped molecules were designed for chemical modification of the surface of probes used for atomic force microscopy (AFM). These chemically functionalized tips were used for chemical force spectroscopy (CFS) measurements of the ligand−protein receptor interaction in a biotin−NeutrAvidin model system. We demonstrate that by using this unique tripodal system, we can achieve significantly lower density of ligand on the AFM tip apex, which is optimal for true single molecule measurements. Furthermore, the molecular tripods form highly stable bonds to the AFM probes, leading to more robust and reproducible unbinding force data, thereby addressing one of the challenges in CFS studies. Histogram analysis of the hundreds of collected unbinding forces showed a specific distribution with a peak force maximum at ∼165 pN, in good agreement with the previously reported data of single rupture events of biotin−avidin. We compared these molecular tripod tips with a molecular monopod. The results showed that the molecular tripods are more robust for repeated measurements. The distinct biotin−avidin force maximum was not observed in the control experiments. This indicated that the force distribution observed for molecular tripods corresponds to the specific rupture force between biotin and avidin. The improved robustness of molecular tripods for CFS will provide benefits in other ligand−receptor unbinding studies, including those of transmembrane receptor systems, which require high resolution, sensitivity, and reproducibility in force spectroscopy measurements.

Introduction

Molecular recognition of noncovalent interactions between small organic molecules and large biomolecules remains an important area of study in chemistry and biology. Especially from the viewpoint of drug design, it is essential to study the intermolecular interactions between small molecules and transmembrane receptors, which are responsible for signal transduction events involved in many diseases. Indeed, almost half of the targeted biomolecules for drug discovery are transmembrane receptors and it is essential to develop techniques to characterize such receptors.[1] Because of the difficulties in obtaining a significant quantity of pure transmembrane protein and the further challenge of preparing single crystals for X-ray studies or high concentrations of such proteins for NMR analysis, the 3-D structure determination of ligand-binding site have hindered classical structure-based approaches to drug discovery.[2] Computer modeling techniques are applicable to many target proteins and are currently an important component of rational drug design. However, this method is based on the 3-D structure of the interacting sites of the protein, which are not available for most transmembrane receptors.

Force spectroscopy has recently emerged as a powerful tool for the study of protein−ligand interactions. The atomic force microscope (AFM), which was originally invented by Binnig and co-workers in the late 1980s,[3] can be applied to both structural and functional analyses of biomolecules.[4] In the structural analysis of proteins, the advantages of AFM include (1) only a small amount of target molecule is necessary for the analysis, (2) measurements can be conducted under biomimetic and physiological conditions, and (3) the protein preparation process is simple. This is particularly beneficial for studies targeting transmembrane receptors, which are difficult to express in large quantities, less soluble due to the hydrophobic transmembrane domains, and therefore difficult to crystallize.[5] In the

*To whom correspondence should be addressed. Telephone: 215-898-3105. Fax: 215-573-4120. E-mail: Yoko.Yamakoshi@uphs.upenn.edu.

(1) Drews, J. *Science* **2000**, *287*, 1960–1964.

(2) (a) Palczewski, K.; Kumasaka, T.; Hori, T.; Behnke, C. A.; Motoshima, H.; Fox, B. A.; Le Trong, I.; Teller, D. C.; Okada, T.; Stenkamp, R. E.; Yamamoto, M.; Miyano, M. *Science* **2000**, *289*, 739–745. (b) Rasmussen, S. G. F.; Choi, H.-J.; Rosenbaum, D. M.; Kobilka, T. S.; Thian, F. S.; Edwards, P. C.; Burghammer, M.; Ratnala, V. R. P.; Sanishvili, R.; Fischetti, R. F.; Schertler, G. F. X.; Weis, W. I.; Kobilka, B. K. *Nature* **2007**, *450*, 383–387. (c) Cherezov, V.; Rosenbaum, D. M.; Hanson, M. A.; Rasmussen, S. G. F.; Thian, F. S.; Kobilka, T. S.; Choi, H.-J.; Kuhn, P.; Weis, W. I.; Kobilka, B.; Stevens, R. C. *Science* **2007**, *318*, 1258–1265. (d) Rosenbaum, D. M.; Cherezov, V.; Hanson, M. A.; Rasmusen, S. G. F; Thian, F. S.; Kobilka, T. S.; Choi, H.-J.; Yao, X.-J.; Weis, W. I.; Stevens, R. C.; Kobilka, B. K. *Science* **2007**, *318*, 1266–1273. (e) Murakami, M.; Kouyama, T. *Nature* **2008**, *453*, 363–367. (f) Bocquet, N.; Nury, H.; Baaden, M.; Le Poupon, C.; Changeux, J.-P.; Delarue, M.; Corringer, P.-J. *Nature* **2009**, *457*, 111–114.

(3) Binnig, G.; Rohrer, H.; Gerber, Ch.; Weibel, E. *Phys. Rev. Lett.* **1986**, *56*, 930–933.

(4) Müller, D. J.; Dufrêne, Y. F. *Nat. Nanotech.* **2008**, *3*, 261–269.

(5) (a) Engel, A.; Müller, D. J. *Nat. Struct. Biol.* **2000**, *7*, 715–718. (b) Scheuring, S.; Fotiadis, D.; Möller, C.; Müller, S. A.; Engel, A.; Müller, D. J. *Single Mol.* **2001**, *2*, 59–67. (c) Müller, D. J.; Hand, G. M.; Engel, A.; Sosinsky, G. *EMBO J.* **2002**, 3598–3607. (d) Müller, D. J.; Engel, A.; Matthey, U.; Meier, T.; Dimroth, P.; Suda, K. *J. Mol. Biol.* **2003**, *327*, 925–930. (e) Seelert, H.; Dencher, N. A.; Müller, D. J. *J. Mol. Biol.* **2003**, *333*, 337–344. (f) Scheuring, A.; Sturigs, J. *Science* **2005**, *309*, 484–487. (g) Nakazawa, K.; Yamakoshi, Y.; Tsuchiya, T.; Ohno, Y. *Eur. J. Pharmacol.* **2005**, *518*, 107–110.

(6) (a) Janshoff, A.; Neitzert, M.; Oberdörfer, Y.; Fuchs, H. *Angew. Chem., Int. Ed.* **2000**, *39*, 3212–3237. (b) Zlatanova, J.; Lindsay, S. M.; Leura, S. H. *Prog. Biophys. Mol. Biol.* **2000**, *74*, 37–61. (c) Hugel, T.; Seitz, M. *Macromol. Rapid Commun.* **2001**, *22*, 989–1016. (d) Rief, M.; Grubmüller, H. *ChemPhysChem* **2002**, 255–261. (e) Ros, R.; Eckel, R.; Bartels, F.; Sischka, A.; Baumgarth, B.; Wiking, S. D.; Pühler, A.; Sewald, N.; Becker, A.; Anselmetti, D. **2004**, *112*, 5−12.(f) Edwardson, J. M.; Henderson, R. H. *Drug Discov. Today* **2004**, *9*, 64–71. (g) Hinterdorfer, P.; Dufrene, Y. F. *Nat. Methods* **2006**, *3*, 347–355. (h) Kienberger, F.; Ebner, A.; Gruber, H. J.; Hinterdorfer, P. *Acc. Chem. Res.* **2006**, *39*, 29–36.

functional analysis of biomolecules, the AFM force−distance curve measurements provide valuable insights into intra- or intermolecular interactions of the target biomolecules.[6] In terms of molecular recognition, AFM can reveal single molecule unbinding events by detecting the rupture force between one ligand molecule and one receptor, thereby revealing information such as dispersion data of individual receptors including dynamic aspects by changing the loading rate. Initial studies of chemical force spectroscopy (CFS) using chemically modified AFM tips[7] have been applied to biological and chemical phenomena including ligand−receptor binding,[8] antigen−antibody interaction,[9] carbohydrate−lectin recognition,[10] protein unfolding,[11] chirality detection,[12] supramolecular host−guest complexation,[13] charge transfer detection,[14] cell−protein interaction,[15] and cell adhesion.[16] These experiments provide data distinct from that obtained by traditional molecular recognition studies using spectroscopic methods such as NMR and UV−vis, which give an ensemble response of all molecules in the experimental system.

In force−distance experiments using CFS, the measurements must be carried out with high resolution, high sensitivity, and high reproducibility. Therefore, improvements of AFM systems are needed to measure reliably the intermolecular interactions between single ligand and single receptor molecules. In a typical experiment of CFS, the ligand molecules are immobilized onto the surface of an AFM tip; therefore, methods of AFM tip modifications are one of the most critical aspects in providing reliable data.[6g] In previous studies using CFS, self-assembled monolayers (SAMs) have been used to functionalize gold-coated silicon or silicon nitride AFM tips. Other methods such as physical protein adsorption, biotin−avidin binding,[8b] and nitrilotriacetic acid−histidine complex formation[17] have also used to assemble molecules on AFM tips. Carbon nanotube-based molecular tips have been found to give more reproducible results with better resolution, but are technically challenging to implement.[8b,18]

In this article, we document a more suitable and convenient method to immobilize ligands onto the AFM tip surface. Our approach provides a stable, organized, and easy-to-use platform for ligand−receptor interaction by employing a synthetic molecular tripod tip for ligand−receptor CFS analysis. Importantly, this approach provides a general method for generating reproducible data and a convenient handle for the covalent attachment of a diverse selection of ligands. We selected gold−sulfur chemistry as the method to attach our organic molecules to the tip of a gold-coated AFM surface using disulfides and thiols. As a stable and rigid scaffold, we have chosen to modify Keana's tetrasubstituted adamantane core[19,20] by adding three sulfur-terminated phenylethynyl legs and a terminal alkyne group as the fourth substituent (Figure 1). This substituted adamantane constitutes the basic scaffold for our molecular tripod tip and makes possible the late-stage functionalization with a ligand (Figure 1a). The advantages of this tripod tip are as follows: (1) strong binding to the gold-coated AFM tip surface through six S−Au bonds; (2) a regular orientation of the molecule with the ligand directed away from the gold surface; (3) lower density of the ligand molecule on the AFM tip apex due to the wide scaffold base, enabling more accurate single molecule experiments; (4) easy modification of the tip with various ligand moieties *via* click chemistry on the terminal acetylene group. As we previously reported, an adamantane-based tripod skeleton has been shown to be stable, rigid, and robust enough for AFM imaging.[21] In this study, we employ a similar tripod scaffold with terminal disulfide groups for ligand−receptor CFS by the addition of a ligand connected to the adamantane scaffold through an ethylene glycol linker suitable for AFM imaging under aqueous conditions (Figure 1a). As an initial study, the CFS measurements of biotin−NeutrAvidin rupture events were carried out using an AFM tip modified with the biotinylated molecular tripod (Figure 2a) and compared to the CFS measurements with the biotinylated molecular monopod tip (Figure 2b), in order to evaluate the molecular tripod for precision and reproducibility of the unbinding forces (Figure 1). The biotin−avidin system was chosen as a model system since this is one of the most well-studied ligand−receptor pairs. Additionally, the biotin−avidin is one of the strongest ligand−receptor interactions, and therefore such a pair should be a suitable for study of the robustness of this CFS system.

Results and Discussion

Synthesis of Molecular Tips. The design of the molecular tip for CFS measurements consisted of three parts (Figure 1a): (1) a tetrasubstituted adamantane "*core*" containing a rigid and spatially wide tripod scaffold, (2) three rigid phenylacetylene "*legs*" terminated with disulfide groups, and (3) an ethylene glycol "*linker*" connecting a ligand to the tripod scaffold. The disulfide groups on the three legs were expected to form six covalent bonds with the gold surface, thereby making a stable attachment of the molecules. This attachment should lead to more reproducible

(7) (a) Lee, G. U.; Lidwell, D. A.; Colton, R. J. *Langmuir* **1994**, *10*, 354–357. (b) Florin, E.-L.; Moy, V. T.; Gaub, H. E. *Science* **1994**, *264*, 415–417. (c) Lee, G. U.; Chrisey, L. A.; Colton, R. J. *Science* **1994**, *266*, 771–773. (d) Frisbie, C. D.; Rozsnyai, L. F.; Noy, A.; Wrington, M. S.; Lieber, C. M. *Science* **1994**, *265*, 2071–2074. (e) Moy, V. T.; Florin, E.-L.; Gaub, H. E. *Science* **1994**, *266*, 257–259.

(8) (a) Allen, S.; Davis, J.; Dawkes, A. C.; Davis, M. C.; Edwards, J. C.; Parker, M. C.; Roberts, C. J.; Sefton, J.; Tendler, S. J. B.; Williams, P. M. *FEBS Lett*. **1996**, *390*, 161–164. (b) Wong, S. S.; Joselevich, E.; Woolley, A. T.; Cheung, C. L.; Lieber, C. M. *Nature* **1998**, *394*, 52–55. (c) Yuan, C.; Chen, A.; Kolb, P.; Moy, V. T. *Biochem*. **2000**, *39*, 10219–10223.

(9) (a) Dammer, U.; Hegner, M.; Anselmetti, D.; Sagner, P.; Dreier, M.; Huber, W.; Guntherodt, H. J. *Biophys. J*. **1996**, *70*, 2437–2441. (b) Harada, Y.; Kuroda, M.; Ishida, A. *Langmuir* **2000**, *16*, 708–715.

(10) Touhami, A.; Hoffmann, B.; Vasella, A.; Denis, F. A.; Dufrêne, Y. F. *Langmuir* **2003**, *19*, 1745–1751.

(11) (a) Rief, M.; Gautel, M.; Oesterhelt, F.; Fernandez, J. M.; Gaub, H. E. *Science* **1997**, *276*, 1109–1112. (b) Fisher, T. M.; Marszalek, P. E.; Fernandez, J. M. *Nat. Struct. Biol*. **2000**, *7*, 719–724. (c) Oberhauser, A. F.; Carrion-Vazquez, M. *J. Biol. Chem*. **2008**, *283*, 6617–6621.

(12) McKendry, R.; Theoclitou, M.-E.; Rayment, T.; Abell, C. *Nature* **1998**, *391*, 566–568.

(13) (a) Schönherr, H.; Beulen, M. W. J.; Bügler, J.; Huskens, J.; van Veggel, F. C. J. M.; Reinhoudt, D. N.; Vanco, G. J. *J. Am. Chem. Soc*. **2000**, *122*, 4963–4967. (b) Auletta, T.; de Jong, M. R.; van Veggel, F. C. J. M.; Huskens, J.; Reinhoudt, D. N.; Zou, S.; Zapotoczny, S.; Shönherr, Vansco, G. J.; Kuipers, L. *J. Am. Chem. Soc*. **2004**, *126*, 1577–1584. (c) Kado, S.; Kimura, K. *J. Am. Chem. Soc*. **2003**, *125*, 4560–4564. (d) Eckel, R.; Ros, R.; Decker, B.; Mattay, J.; Anselmetti, D. *Angew. Chem., Int. Ed*. **2005**, *44*, 484–488. (e) Schäfer, C.; Decker, B.; Letzel, M.; Novara, F.; Eckel, R.; Ros, R.; Anselmetti, D.; Mattay, J. *Pure Appl. Chem*. **2006**, *78*, 2247–2259. (f) Schäfer, C.; Eckel, R.; Ros, R.; Mattay, J.; Anselmetti, D. *J. Am. Chem. Soc*. **2007**, *129*, 1488–1489. (g) Anselmetti, D.; Bartels, F. W.; Becker, A.; Decker, B.; Eckel, R.; McIntosh, M.; Mattay, J.; Plattner, P.; Ros, R.; Schäfer, C.; Sewald, N. *Langmuir* **2008**, *24*, 1365–1370.

(14) Skulason, H.; Frisbie, C. D. *J. Am. Chem. Soc*. **2002**, *124*, 15125–15133.

(15) Bustanji, Y.; Arciola, C. R.; Conti, M.; Mandello, E.; Montanaro, L.; Samori, B. *Proc. Natl. Acad. Sci. U.S.A*. **2003**, *100*, 13292–13297.

(16) Evans, E. A.; Calderwood, D. *Science* **2007**, *316*, 1148–1153.

(17) Riener, C. K.; Kienberger, F.; Hahn, C. D.; Buchinger, G. M.; Egwin, I. O. C.; Haselgrübler, T.; Ebner, A.; Romanin, C.; Klampfl, C.; Lackner, B.; Prinz, H.; Blass, D.; Hinterdorfer, P.; Gruber, H. *Anal. Chim. Acta* **2003**, *497*, 101–114.

(18) (a) Woolley, A. T.; Cheung, C. L.; Hafner, J. H.; Lieber, C. M. *Chem. Biol*. **2000**, *7*, R193–R204. (b) Hafner, J. H.; Cheung, C. L.; Woolley, A. T.; Lieber, C. M. *Prog. Biophys. Mol. Biol*. **2001**, *77*, 73–110.

(19) (a) Yao, Y.; Tour, J. M. *J. Org. Chem*. **1999**, *64*, 1968–1971. (b) Deng, X.; Cai, C. *Tetrahedron Lett*. **2003**, *44*, 815–817. (b) Nikitin, K.; Lestini, E.; Lazzari, M.; Altobello, S.; Fitzmaurice, D. *Langmuir* **2007**, *23*, 12147–12153.

(20) (a) Li, Q.; Rukavishnikov, A. V.; Petukhov, P. A.; Zaikova, T. O.; Keana, J. F. W. *Org. Lett*. **2002**, *21*, 3631–3634. (b) Li, Q.; Rukavishnikov, A. V.; Petukhov, P. A.; Zaikova, T. O.; Jin, C.; Keana, J. F. W. *J. Org. Chem*. **2003**, *68*, 4862–4869.

(21) Takamatsu, D.; Yamakoshi, Y.; Fukui, K. *J. Phys. Chem. B* **2006**, *110*, 1968–1970.

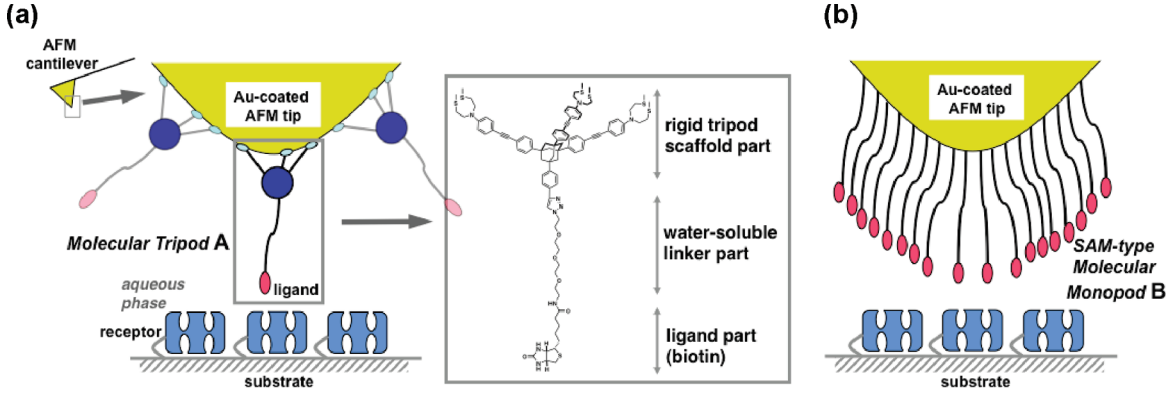

Figure 1. (a) Design of a molecular tripod tip **A** for ligand−receptor AFM force spectroscopy and (b) comparison with a molecular monopod tip **B** system. Because of the wider base of the molecular tripod **A**, the density of the molecules on the modified AFM tip surface is lower than with monopod **B**, enabling a higher probability of single molecule measurements. The attachment of the molecular tripod **A** through the three disulfide legs provides more stable immobilization of the molecule, giving more robust chemically modified probes.

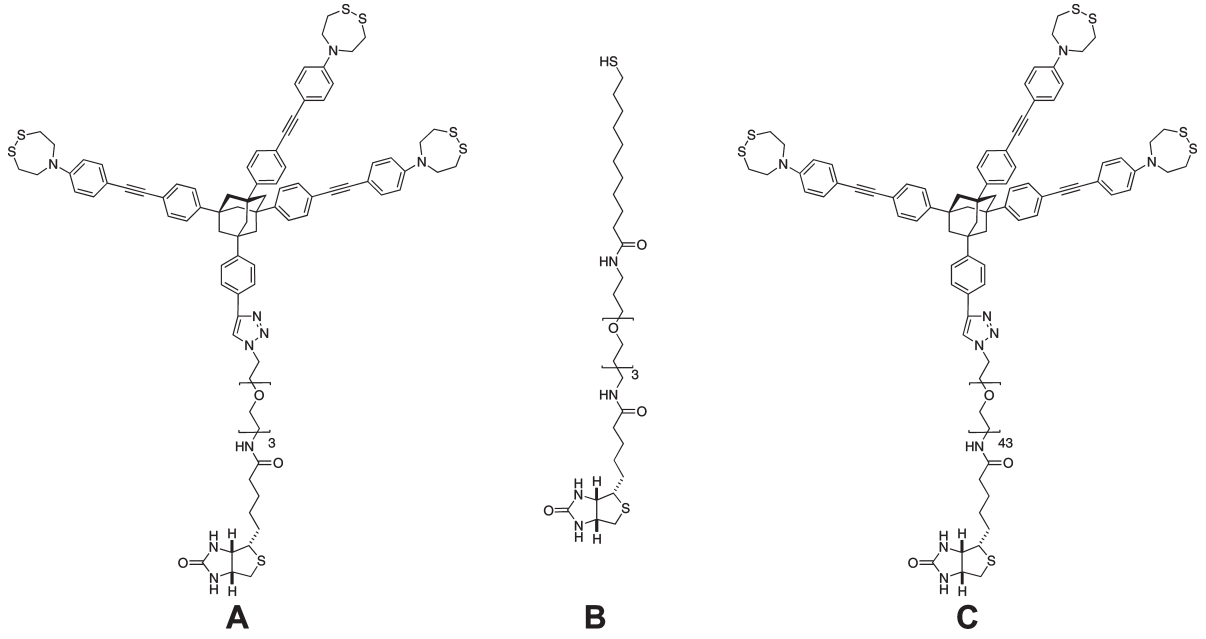

Figure 2. Structures of the three biotinylated molecules for chemical force spectroscopy: molecular tripod **A**, molecular monopod **B**, and long molecular tripod **C**.

data by surviving repeated force curve measurements better.[22,23] One of the key requirements for the ligand−receptor interaction measurements by CFS is that the AFM tip modification has to be mechanically robust to withstand several hundreds of repeated measurements. The large and rigid foundation of the tripod scaffold is advantageous for the orientation of the ligand perpendicular to the gold surface and farthest from the AFM tip. It also offers a lower density of ligand molecules on the AFM tip surface, which should provide better single molecule interaction data (Figure 1a). The ethylene glycol chain, which is soluble and flexible in aqueous media, was chosen as a suitable linker for CFS measurements in water.

In this study, three molecular tips **A**−**C** (Figure 2) were prepared by convergent synthesis and assembly of the core, legs, linker, and ligand. Molecular tripod **A** and monopod **B** were synthesized to evaluate the advantages of the tripod skeleton by comparing the precision and reproducibility in the force measurements with both molecular tips. Additionally, tripod **C** with a longer poly(ethylene glycol) linker between the core and ligand was prepared to analyze the effect of the length of the linker chain, as it has been reported that a longer linker will provide higher mobility of the ligand and narrower lateral resolution of the target site.[24]

The synthesis of molecular tripod **A** was carried out as shown in Schemes 1 and 2 by modification of Keana's procedures. The tripod scaffold was prepared by Sonogashira couplings starting from 1,3,5,7-tetrakis(4-iodophenyl)adamantane (**1**) (Scheme 1). The adamantane **1** was functionalized with a single TIPS-acetylene to give **2**. Three ethynylphenyldithiazepanes (**3**) were added to give **4**, constituting the tripod skeleton. The TIPS-acetylene group of **4** was deprotected with TBAF to give terminal acetylene **5**, which was poised for further functionalization.

(22) Nuzzo, R. G.; Allara, D. L. *J. Am. Chem. Soc.* **1983**, *105*, 4481–4483.
(23) Biebuyck, H. A.; Bain, C. D.; Whitesides, G. M. *Langmuir* **1994**, *10*, 1825–1831.
(24) Kienberger, F.; Ebner, A.; Gruber, H. J.; Hinterdorfer, P. *Acc. Chem. Res.* **2006**, *39*, 29–36.

Scheme 1. Synthesis of Tripodal Scaffold for the Molecular Tripod Tip A[a]

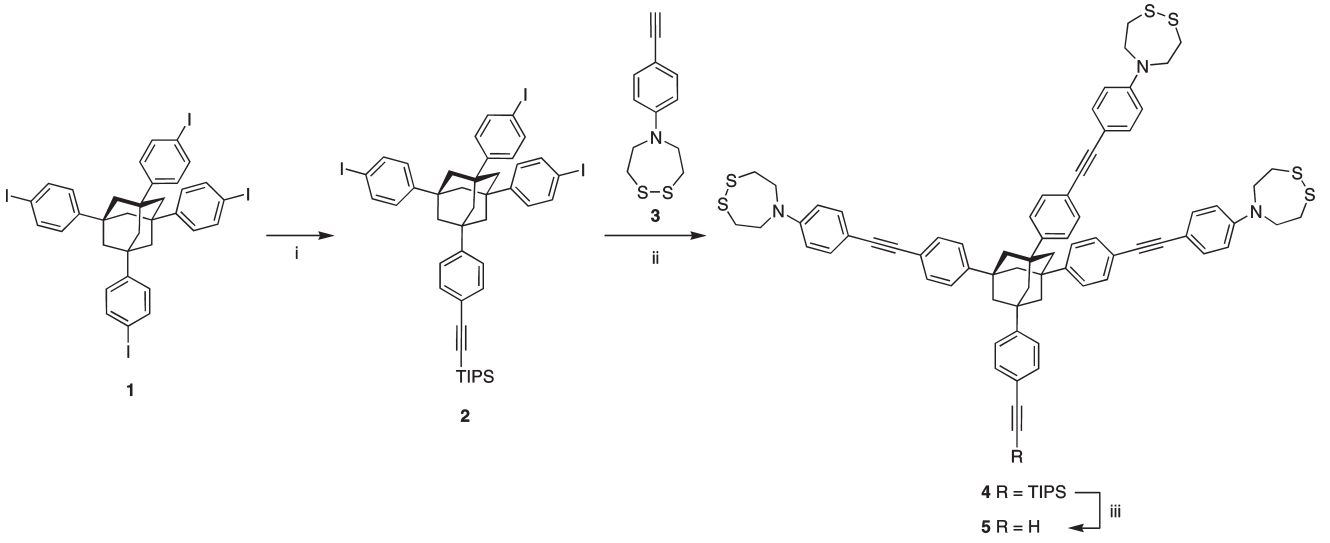

[a] Reagents and conditions: (i) TIPS−acetylene, $Pd(PPh_3)_2Cl_2$, PPh_3, CuI, Et_3N/THF, room temperature, 18%; (ii) **3** (3 equiv), $Pd(PPh_3)_2Cl_2$, PPh_3, CuI, Et_3N/THF, room temperature, 51%; (iii) TBAF, THF, room temperature, 90%.

The linker **6** containing an azide and a primary amine was prepared from tetraethylene glycol.[25] An HBTU coupling of linker **6** with biotin provided the ligand−linker conjugate **7**, which was subsequently attached to tripod scaffold **5**. The Sharpless click chemistry reaction conditions with $CuSO_4$ and ascorbic acid in $H_2O-{}^tBuOH$ at room temperature[26] did not provide the desired product, presumably due to the low solubility of **5** in this solvent system. Instead, the procedure reported previously by Meldal and co-workers with CuI and DIPEA in degassed THF at 60 °C provided molecular tip **A** in good yield (Scheme 2).[27]

The molecular monopod **B** was synthesized based on the reported protocol with slight modifications.[28,29] The synthesis of molecular tripod **C** with the longer poly(ethylene glycol) chain was carried out in a similar manner to the synthesis of tripod **A**.

Chemical Modification of the AFM Tip and Force Measurements. AFM force measurements were performed using an Asylum Research molecular force probe. Separate experiments were performed with molecular tips **A**, **B**, and **C**. Using the well-established binding of disulfides and thiols with gold, molecular tips **A** and **B** were immobilized on the surface of gold-coated AFM tip apex *via* covalent bonds. Cleaned, commercially available gold-coated AFM cantilevers were soaked overnight in a filtered DMSO solution (100 μM) of **A**, **B**, or **C**.[30] Each cantilever was washed with DMSO, ethanol, and water five times each to remove unbound molecules. The modified AFM tips were mounted for force spectroscopy measurements. Commercially available agarose beads (size 40−165 μm) with covalently bound

Scheme 2. Conjugation of Tripod Scaffold 5 with Ligand−Linker 7 To Give the Molecular Tripod Tip A[a]

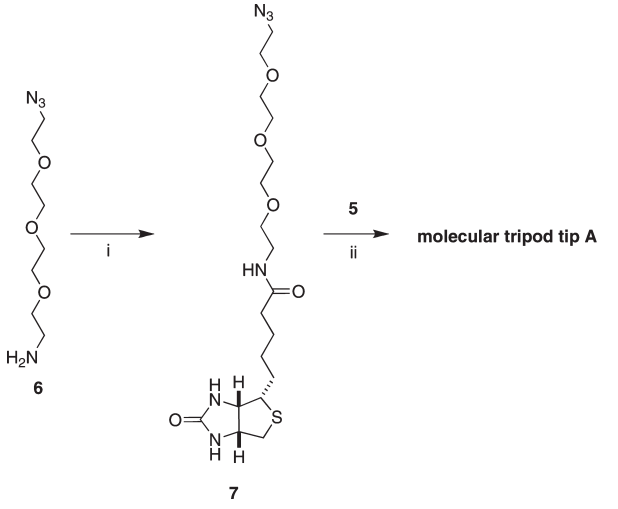

[a] Reagents and conditions: (i) D-Biotin, HBTU, DIPEA, DMF, 76%; (ii) CuI, DIPEA, THF, 60 °C, 85%.

NeutrAvidin were used as the receptor substrate.[31] NeutrAvidin is a deglycosylated avidin protein which exhibits exceptionally low nonspecific binding interactions.[32] All force measurements were carried out in 20 mM HEPES buffer (pH 7.4) and repeated several hundred times for each experiment. Each cantilever was calibrated using the thermal noise method before and after the modification of tip.[33]

As illustrated in Figure 1, tripod **A** is expected to yield a lower density of ligand molecules on the surface compared to monopod **B** due to its wider base. In the first round of experiments, 500−600 force measurements were carried out using each molecular tip

(25) Schwabacher, A. W.; Lane, J. W.; Schiesher, M. W.; Leigh, K. M.; Johnson, C. W. *J. Org. Chem.* **1998**, *63*, 1727–1729.
(26) Rostovtsev, V. V.; Green, L. G.; Fokin, V. V.; Sharpless, K. B. *Angew. Chem., Int. Ed.* **2002**, *41*, 2596–2599.
(27) Tornoe, C. W.; Christensen, C.; Meldal, M. *J. Org. Chem.* **2002**, *67*, 3057–3064.
(28) (a) Nelson, K. E.; Gamble, L.; Jung, L. S.; Boeckl, M. S.; Naeem, E.; Golledge, S. L.; Sasaki, T.; Castner, D. G.; Campbell, C. T.; Stayton, P. S. *Langmuir* **2001**, *17*, 2807–2816. (b) Shumaker-Parry, J. S.; Zareie, M. H.; Aebersold, R.; Campbell, C. T. *Anal. Chem.* **2004**, *76*, 918–929.
(29) Detail of the synthesis of molecular tip **B** is written in Supporting Information.
(30) After preliminary trials of soaking in other solutions such as $CHCl_3$ and THF, DMSO was selected as a solvent that provided enough solubility for all of molecular tips **A**−**C**. Also, preliminary data with 2 h of soaking of the AFM tip in a DMSO solution of molecular tip **A** did not give enough rupture events for analysis.
(31) Initially we attempted to use other avidin-modified surfaces. Force spectroscopy experiments with streptavidin bound to mica and covalently bound to glass cover slips yielded no conclusive results. These substrate were probably too rigid for pulling experiments, and mostly strong desorption peaks were evident upon retraction of the tip from the surface.
(32) Hiller, Y.; Gershoni, J. M.; Bayer, E. A.; Wilchek, M. *Biochem. J.* **1987**, *248*, 167–171.
(33) Hutter, J. L.; Bechhoefer, J. *Rev. Sci. Instrum.* **1993**, *64*, 1868–1873.

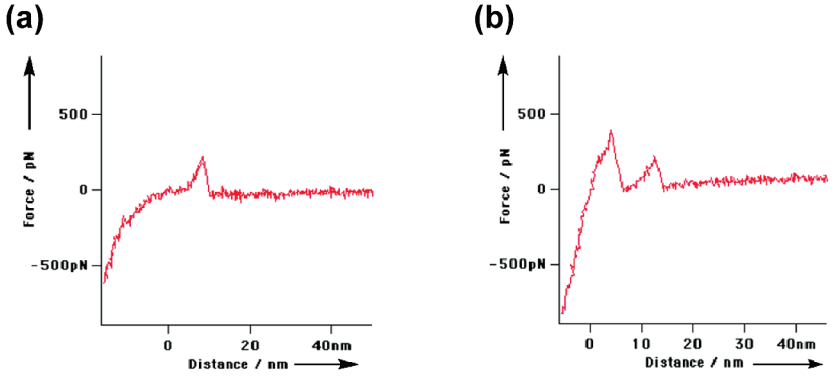

Figure 3. Typical force versus distance curves using molecular tripod tip **A** against NeutrAvidin-linked agarose beads. Representative force curves of a single rupture event (a) and multiple molecular events (b) in one approach. All measurements were carried out in 20 mM HEPES buffer (pH 7.4) with a scan rate of 0.12 Hz, a tip velocity of 500 nm/s, a distance of 2 μm, and a loading rate of 1.0×10^5 pN/s. The spring constant of each cantilever was calibrated before and after each measurement. Since the receptor is immobilized on compressible beads, the absolute distance is not accurate.

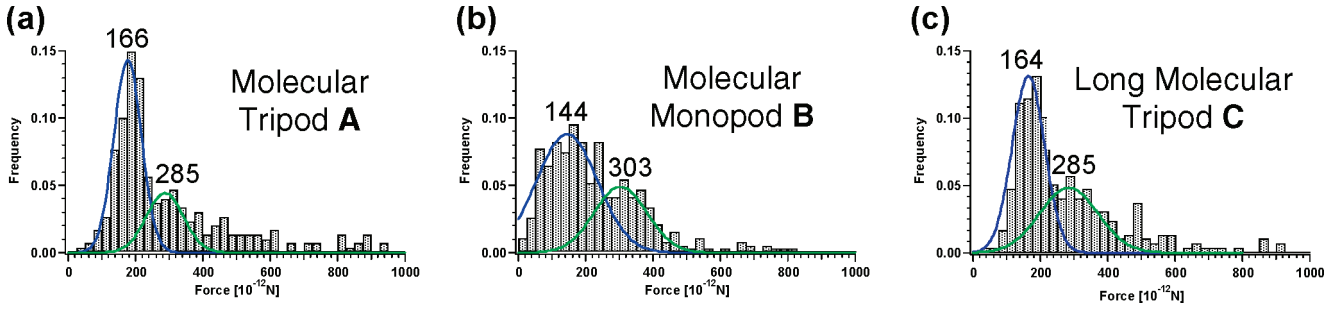

Figure 4. Histogram analysis of rupture force distributions between biotin and NeutrAvidin: (a) using molecular tripod tip **A**. The centers of the force distributions are at 166 and 285 pN (with 165 measurements and 247 observed rupture peaks); (b) using molecular monopod tip **B**. The centers are at 144 and 303 pN (with 178 measurements and 392 observed rupture peaks); (c) using longer-linker molecular tripod tip **C**. The centered at 164 and 285 pN (with 180 measurements and 348 observed rupture peaks). Calculated loading rates were 1.0×10^5, and 6.4×10^4, and 9.9×10^4 pN/s for each functionalized tip. The blue and green lines are Gaussian fits of the histograms. The frequencies were calculated based on the total observations with rupture forces below 1000 pN.

(**A**, **B**, or **C**). In the experiment with tripod **A**, 29% of the measurements had detectable rupture forces, as compared with monopod **B** (37%) and longer tripod **C** (38%).[34] Figure 3 shows typical force−distance curves of biotin−NeutrAvidin unbinding measurements using tripod **A** that correspond to single- (Figure 3a) and double-rupture events (Figure 3b). Most of the experiments with **A**, **B**, and **C** exhibited these two types of force curves, with an additional small amount of multiple rupture events. The average number of force peaks observed in pulls with peaks was 1.7 for tripod **A**, 2.2 for monopod **B**, and 1.9 for longer tripod **C**.

Comparison of Unbinding Force Distribution between Tripod and Monopod. From the observed force−distance curves, the magnitude of the rupture forces were analyzed. Histograms are shown in Figure 4, parts a, b, and c, for tripod **A**, monopod **B**, and longer tripod **C**, respectively. Results for molecular tips **A** and **C** showed the main rupture force at 166 and 164 pN, respectively (blue lines in Figure 4). These rupture force maxima lie close to the 160 pN force value reported for a single biotin−avidin rupture event,[35] suggesting that these peaks correspond to a single molecule rupture force. Monopod tips **B** showed a lower mean rupture force (144 pN) and a broader force distribution than tripod tips **A** and **C**. The tripod tips **A** and **C** give more reproducible rupture forces than the monopod tip **B**. A second force peak with larger rupture forces was observed with all 3 types of tips (green lines in Figure 4). These peaks all had mean rupture forces within 10% of each other.

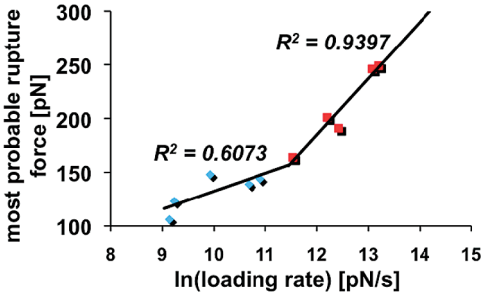

Figure 5. Loading rate dependency of the most probable rupture force of tripod **A**-modified AFM tip and a NeutrAvidin-bound agarose bead substrate. The diagram shows two regimes during unbinding: the blue and red points can be assigned to the inner and outer barriers.[35,39]

In many experimental force curves, a large desorption force peak, as well as relatively strong multimolecular rupture events, were observed prior to the last event, which had a relatively small rupture force. As the AFM tip is removed from the surface, the last detected interactions are most likely between the biotin bound to the molecular tip and NeutrAvidin bound to the surface.[36]

(34) Detailed data is shown in the Supporting Information.
(35) Merkel, R.; Nassoy, P.; Leung, A.; Ritchie, K.; Ecans, E. *Nature* **1999**, *397*, 50–53.
(36) Fantner, G. E.; Oroudjev, E.; Schitter, G.; Golde, L. S.; Thurner, P.; Finch, M. M.; Turner, P.; Gutsmann, T.; Morse, D. E.; Hansma, H.; Hansma, P. K. *Biophys, J.* **2006**, *90*, 1411–1418.

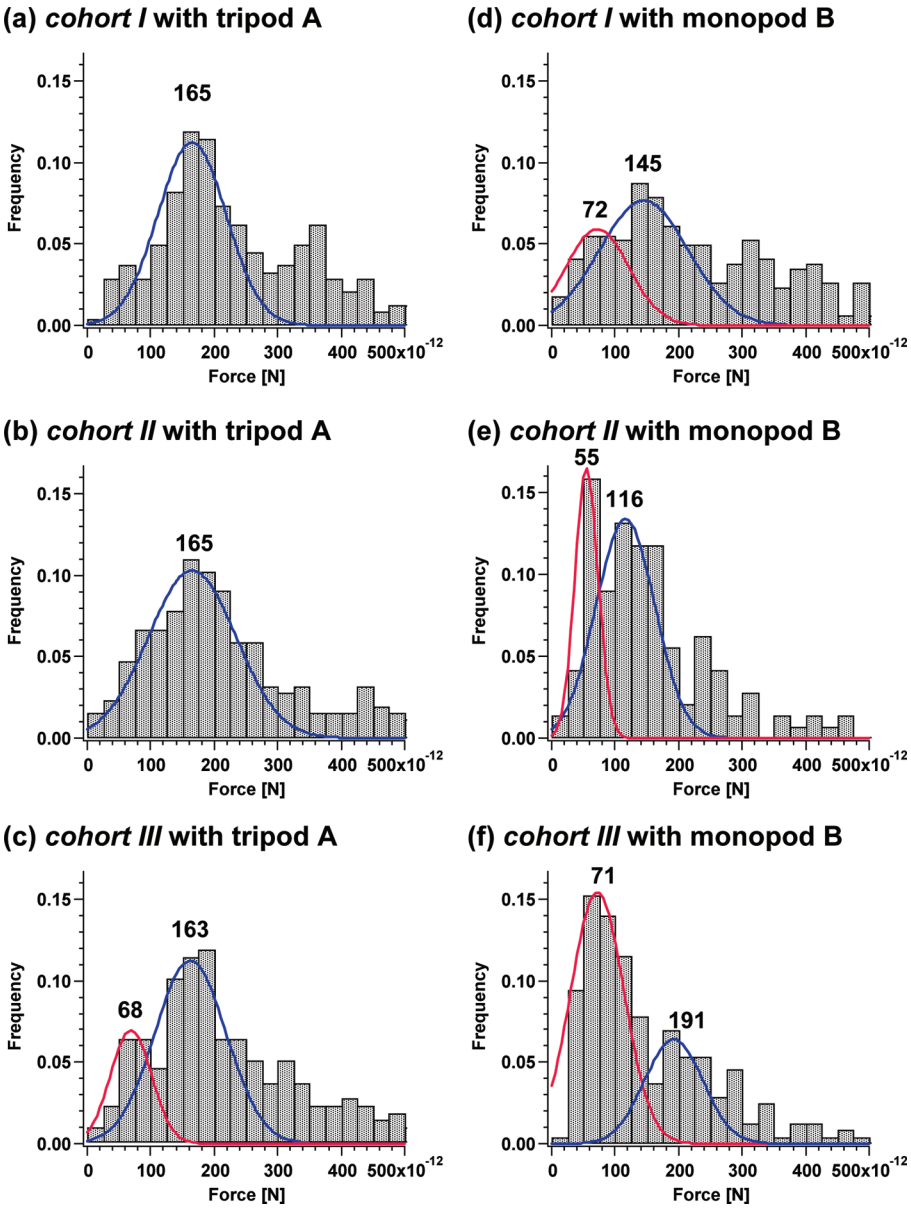

Figure 6. Robustness of the molecular tips. Histograms show rupture peaks in 600 continuous cycles using a single AFM tip functionalized with tripod **A** (a−c) or monopod **B** (d−f). The 600 cycles were divided into three cohorts; the cycles 0−200 (*cohort I*, for tripod **A** (a) and monopod **B** (d)), cycles 201−400 (*cohort II*, for **A** (b) and for **B** (e)), and cycles 401−600 (*cohort III*, for **A** (c) and for **B** (f)). The numbers at the centers of the distribution are from Gaussian fits to the histograms corresponding to the single molecule rupture event (blue lines) and the observed nonspecific rupture forces (red lines). Monopod **B** shows inconsistency in the mean rupture forces for single rupture events and many nonspecific low-force ruptures. Tripod **A** shows stable and constant distribution curves over the repeated measurements. The frequencies were calculated based on the total number of observations with rupture forces below 1000 pN and the expanded histogram below 500 pN is shown.

Therefore we extracted data only from the last rupture events of each measurement, which are expected to be single rupture forces.[37] As a result of this analysis, the second peak corresponding to multiple rupture events in the measurement with tripod **A** largely disappeared, whereas the same peak still existed in the experiments with monopod **B** and longer tripod **C**. Additionally, experiments with the most probable rupture force dependency on the loading rate were carried out and gave almost identical data to the previously reported values (Figure 5).[35,38]

Because hundreds of cycles are needed to provide the necessary statistical data for conclusive results in a force spectroscopy experiment, it is expected that damage to the chemically modified tip will occur during repeated measurements. Possibilities of damage include mechanical stress, oxidative cleavage of S−Au bonds, and exchange of the monolayer on the gold surface.[40] Thus, the robustness of the functionalized AFM tips becomes essential for the results of CFS experiments. As described above, we hypothesized that the tripod tips, which are bound to the AFM tip through multiple points, could better withstand these stresses.

(37) Detailed data is shown in the Supporting Information.
(38) Pincet, F.; Husson, J. *Biophys. J.* **2005**, *89*, 4374–4381.
(39) Yuan, C.; Chen, A.; Kolb, P.; Moy, V. T. *Biochemistry* **2000**, *39*, 10219–10223.
(40) (a) Schlenoff, J. B.; Li, M.; Ly, H. *J. Am. Chem. Soc.* **1995**, *117*, 12528–12536. (b) Yang, W.; Auciello, O.; Butler, J. E.; Cai, W.; Carlisle, J. A.; Gerbi, J. E.; Gruen, D. M.; Knickerbocker, T.; Lasseter, T. L.; Russel, J. N.; Smith, L. M.; Hamers, R. J. *Nat. Mater.* **2002**, *1*, 253–257.

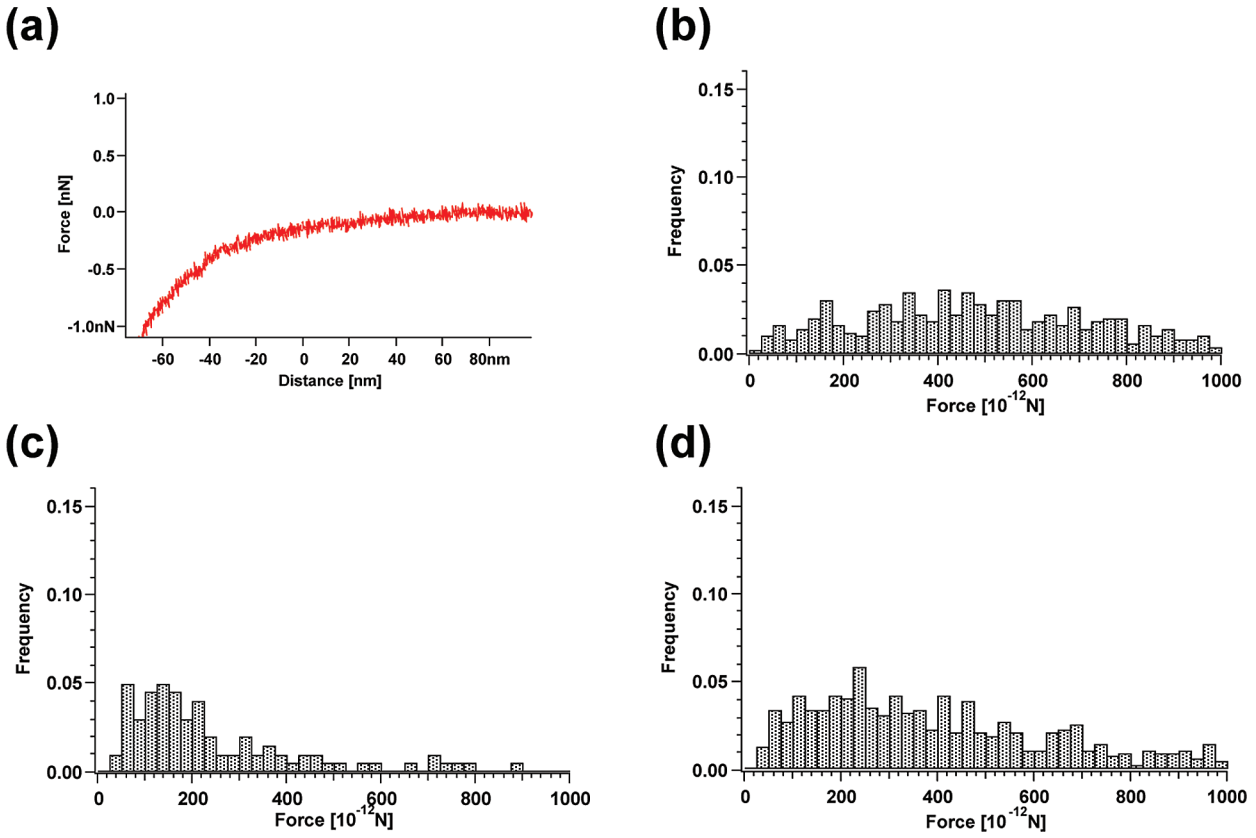

Figure 7. Control experiments of force measurements between an unfunctionalized tip and NeutrAvidin substrate (a) typical force curve; (b) force histogram), (c) between a functionalized tip with tripod **A** and agarose beads lacking NeutrAvidin, and (d) between a functionalized tip with tripod **A** and NeutrAvidin substrate in the presence of excess free biotin in the solution.

This hypothesis was tested by comparing the robustness of the tripod and the monopod tips. In these experiments, 600 continuous measurements were taken with molecular tips **A** and **B** and were divided into three *cohorts I*−*III* (the first 200 cycles, the second 200, and the third 200). The resulting forces in each cohort were plotted in force histograms for tripod **A** (Figures 6a−c) and monopod **B** (Figures 6d−f).

The force measurements with an AFM tip functionalized with tripod **A** showed a force maximum at ∼165 pN peaks for all three parts (*cohorts I*−*III*) corresponding to single biotin−avidin rupture events (Figure 6a−c). Only in the last cohort (*III*), was a small peak of lower force observed (the red curve with a peak maximum at 68 pN), indicating nonspecific unbinding forces by a damaged tip or substrate. In contrast, the results with monopod **B** show significant variations in the force maxima for single molecule rupture forces in the histograms. Especially in *cohorts II* and *III*, new large peaks at lower rupture forces were observed (50−80 pN; red curves in Figure 6e−f). The appearance of these lower forces and their predominance in the force histograms can be attributed to a change in the surface properties of the tip. The shift toward smaller rupture forces is indicative of nonspecific forces, which are unrelated to ligand−receptor rupture. This interaction could be caused by a hydrophobic attraction of the partially damaged layer of organic molecules on the surface of the tip toward the substrates. The tripod force histograms remain constant throughout the duration of the experiment because of the tripod′s increased stability.

Control Experiments. To confirm that the observed force distribution peaks in the experiments with tripod **A** correspond to the specific rupture events of the biotin ligand present on the molecular tip and protein on the substrate, three control force experiments were carried out: (1) experiments using an unfunctionalized AFM tip; (2) an experiment using a substrate of agarose beads lacking the avidin protein; (3) an experiment with an excess of free biotin present in the solution. For control experiment 3, the NeutrAvidin-coated beads were soaked overnight in a biotin solution so that all free binding sites of the protein were saturated. The results of these control experiments are shown in Figure 7. There was no significant force maximum in any range of force in all of the control experiments. Although there are some rupture forces in the range 50−250 pN in experiment 2, the distribution was very broad and the measurement of any observed forces were too few to give reliable data (Figure 7c). In the quenching experiment (control experiment 3) in the presence of excess free biotin, 90% of measurements gave some force peak, with 3.2 peaks on average per measurement, indicating that the modified tip with **A** exhibited many interactions between the organic molecule on the AFM tip and the substrate protein. Fewer peaks were observed in control experiments lacking either ligand or receptor. Even though many rupture forces were observed in control experiment 3, there was no specific force maximum that can be associated with ligand−receptor interaction (Figure 7d). These control experiments confirm that the distinct forces centered at 165 pN in the study with tripod **A** are specific to the single molecule interactions between biotin and NeutrAvidin.

Conclusions

Three biotinylated compounds **A**−**C** were synthesized as molecular tips for chemical modification of AFM tips and CFS measurements. The molecular tripod tips were synthesized by taking advantage of a tetrasubstituted adamantane core featuring

three rigid phenylethynyl legs and a fourth group containing a terminal acetylene. The terminal acetylene can be easily modified by a 1,3-dipolar cycloaddition with an azide group. Two molecular tripods **A** and **C** with different linker lengths were prepared. For comparison, molecular monopod **B** with an alkyl thiol scaffold and ethylene glycol linker terminated with a biotin ligand was also synthesized. These three biotinylated molecular tips **A**, **B**, and **C** were adsorbed onto gold surfaces of AFM tips and successfully employed in force−distance curve measurements with a NeutrAvidin substrate. The single molecule rupture events were clearly observed in the experiments with molecular tripod tips (**A**, with shorter linker and **C**, with longer linker), with significantly sharper force distributions, as compared to the results with molecular monopod tip **B**, indicating that the rigid tripod scaffold with adamantane−acetylene structure is highly advantageous for CFS. The force values obtained in this study are in good agreement with previously reported results. The length of the linker in molecular tripod tips did not affect significantly the distribution of rupture forces. Furthermore, the robustness of the tripod and monopod tips for CFS was compared by continuously repeated measurements. We demonstrated that, as observations are accumulated during the repeated approach/retract cycles, the distribution of the rupture forces for the monopod system is rapidly altered toward nonspecific interactions, whereas the tripods provide consistent results throughout the experiments. We hypothesize this reproducibility is because of the strong connection of the molecular tripod tip onto the gold surface through multiple (six) covalent S−Au bonds in the tripod legs. Complementary results of the control experiments demonstrated that the majority of the observed rupture force distribution peaks in molecular tripod tips correspond to the specific unbinding force of biotin and NeutrAvidin. The molecular tripod tips will be useful for AFM tip modification with various ligands for CFS measurements. Currently, the terminal alkyne group of the tripod scaffold is being applied to *in situ* modification of the AFM tip through click reaction with various kinds of ligand molecules, toward the development of high throughput drug screening, and studies of transmembrane receptors.

Experimental Section

Synthesis of the Biotinylated Molecular Tips for AFM Tip Modification. *General Data*. Melting points were measured with MELTEMP (Laboratory Devices, Holliston, MA) and are uncorrected. ^{1}H and ^{13}C NMR spectra were recorded on a Varian 400 NMR spectrometer (Varian Inc., Palo Alto, CA) at 400 and 100 MHz, respectively. Mass spectrometry was performed on the VG70 doublefocusing mass spectrometer (VG Analytical, Manchester, U.K.) for the ionization methods of electron impact (EI), chemical ionization (CI), and fast atom bombardment (FAB). Electrospray ionization (ESI) MS was performed on the PE Sciex Qstar (Applied Biosystems, Foster City, CA) and matrix assisted laser desorbed ionization-time-of-flight (MALDI−TOF) MS was performed on MALDI−TOF DYNAMO system (Thermo Bioanalysis Corp., Santa Fe, NM). The IR was recorded on the FT/IR-430 (JASCO, Tokyo, JPN). All the reagents were purchased from the corresponding commercially available sources and purified as described when needed. All solvents were purchased from EMD Chemicals Inc. (Gibbston, NJ) unless otherwise noted. THF, acetonitrile, and methanol were passed over activated alumina under an Ar atmosphere and DMF was passed over molecular sieves under an Ar atmosphere by a solvent system (Innovative Technology Inc., Newburyport, MA). Benzene and dichloromethane were distilled over calcium hydride. Column chromatography, analytical TLC, and preparative TLC were performed on Silica Gel (Merck Silicagel 60 F254 (Art 5715) 0.25 mm, EM Science silica gel 60 PF254, and E. Merck Silica gel 60 (230−400 mesh), respectively). TLC plates were visualized by UV light, a phosphomolybdic acid stain, or a $KMnO_4$ stain.

Synthesis of Triisopropyl[4-[3,5,7-tris-(4-iodophenyl)adamantan-1-yl]phenylethynyl]silane (**2**). In a solution of **1** (1.28 g, 1.36 mmol) in THF (10 mL), $Pd(PPh_3)_2Cl_2$ (48 mg, 0.068 mmol), CuI (5 mg, 0.03 mmol), PPh_3 (8 mg, 0.03 mmol), and Et_3N (5 mL) were added in a Schlenk tube and the reaction mixture was degassed four times by freeze−pump−thaw. After the addition of triisopropylsilylacetylene (Fluka, 0.152 mL), the reaction mixture was degassed once more and was stirred at room temperature overnight in Ar atmosphere. The reaction mixture was concentrated *in vacuo* and the crude mixture was purified by silica gel flash column chromatography (hexane−$CHCl_3$ (5:1)) twice to give colorless crystals **2** (0.250 g, 0.250 mmol, y = 18%): R_f = 0.43 (hexane−chloroform (5:1)); mp 182−185 °C; IR (thin film) 3087, 3046, 2938 (s), 2897, 2862 (s), 2154, 1898, 1504, 1487 (s), 1462, 1449, 1391, 1357, 1263, 1068, 1189, 1003 (s), 883, 835, 818, 779, 739, 705, 679, 662; ^{1}H NMR (400 MHz, $CDCl_3$) δ 7.68 (d, J = 8.4 Hz, 6H, Ar***H*** *ortho* to iodine), 7.48 (d, J = 8.4 Hz, 2H, Ar***H*** *ortho* to −TIPS alkyne), 7.37 (d, J = 8.3 Hz, 2H, Ar***H*** *meta* to TIPS alkyne), 7.21 (d, J = 8.6 Hz, 6H, Ar***H*** *meta* to iodine), 2.08 (s, 12H, adamantane), 1.14 (s, 21H, −TIPS group); ^{13}C NMR (100 MHz, $CDCl_3$) δ 149.10, 148.68, 137.69, 132.35, 127.35, 125.01, 121.82, 106.99, 91.91, 90.70, 46.90, 46.85, 39.38, 39.24, 18.87, 11.49; MS(FAB) m/z calcd for $C_{45}H_{49}I_3Si$ = 998, found = 998 (M^+), 955 ($[M - C_3H_7]^+$).

Synthesis of Triisopropyl[4-[3,5,7-tris-[4-[4-(1,2,5-dithiazepan-5-yl)phenylethynyl]phenyl]adamantan-1-yl]phenylethynyl]silane (**4**). A THF solution (15 mL) of compound **2** (0.486 g, 0.487 mmol), compound **3** (0.500 g, 2.13 mmol), $Pd(PPh_3)_2Cl_2$ (24 mg, 0.034 mmol), PPh_3 (13 mg, 0.05 mmol), and Et_3N (5 mL) in Schlenk tube was thoroughly degassed by freeze−pump−thaw before CuI (20 mg, 0.105 mmol) was added. The reaction mixture was degassed again and was stirred at room temperature for 2 days and subsequently at 60 °C for 4 h. The reaction mixture was concentrated *in vacuo* and the resulting mixture was dissolved in CH_2Cl_2 (100 mL) and washed with 1 M HCl (50 mL) and NH_4OH-NH_4Cl (9:1, v/v, 50 mL) twice to remove any remaining copper. The reaction mixture was then purified by silica gel column chromatography to give a powdery brown solid, **4** (325 mg, 0.246 mmol, y = 51%): R_f = 0.48 (toluene−hexane (5:1)); mp > 210 °C (dec); IR (thin film) 3081, 3039, 2924, 2861, 2209, 2153, 1602, 1521 (s), 1468, 1398, 1352, 1285, 1216, 1167, 1138,1014, 900, 815; ^{1}H NMR (400 MHz, $CDCl_3$) δ 7.39 − 7.53 (m, 22 H, Ar***H***), 6.60 (d, J = 9.1 Hz, 6H, Ar***H*** *ortho* to amine), 3.99 (t, J = 5.5 Hz, 12H, $-NCH_2C\boldsymbol{H_2}SS-$), 3.10 (t, J = 5.5 Hz, 12 H, $-NC\boldsymbol{H_2}CH_2SS-$), 2.16 (s, 6H, adamantane), 2.14 (s, 6H, adamantane), 1.14 (s, 21H, −TIPS group); ^{13}C NMR (100 MHz, $CDCl_3$) δ 148.73, 146.47, 137.70, 133.39, 132.31, 131.56, 127.33, 125.21, 125.16, 122.11, 111.34, 110.77, 91.93, 90.47, 90.25, 87.59, 52.64, 47.06, 39.45, 36.95, 18.89, 11.52; MS(FAB) m/z calcd for $C_{81}H_{85}N_3S_6Si$ = 1319, found = 1320 ($[M + H]^+$).

Synthesis of Scaffold Part (**5**). To a solution of **4** (0.200 g, 0.152 mmol) in THF (5 mL), which was dissolved by sonication, a 1.0 M solution of TBAF (Sigma-Aldrich, 0.160 mL, 0.16 mmol) in THF was added at room temperature. When there was no starting material detected by TLC, the solution was concentrated *in vacuo* to dryness. The solid was dissolved in CH_2Cl_2 (50 mL) and washed with NH_4Cl (15 mL). The organic layer was dried over Na_2SO_4 and filtered through a plug of silica. The filtrate was then concentrated *in vacuo* to give a yellowish solid. Et_2O (20 mL) was added to the solid and sonicated for 10 min. The supernatant liquid was removed by pipet and disposed. This process was repeated two more times to give a yellowish powder **5** (160 mg, 0.137 mmol, y = 90%): mp > 260 °C; IR (KBr) 3287, 3080, 3035, 2925, 2851, 2204, 1604 (s), 1520 (s), 1398, 1352 (s), 1216, 1180, 1166, 1138, 1012, 900, 814, 645, 555, 526; ^{1}H NMR (400 MHz, $CDCl_3$) δ 7.38−7.53 (m, 22H, Ar***H***), 6.60 (d, J = 8.9 Hz, 6H, Ar***H***

ortho to amine), 3.99 (t, J = 5.5 Hz, 12 H, $-NCH_2CH_2SS-$), 3.10 (t, J = 5.5 Hz, 12H, $-NCH_2CH_2SS-$), 3.07 (s, 1H, terminal alkyne) 2.16 (s, 12H, adamantane); ^{13}C NMR (100 MHz, $CDCl_3$) δ 148.67, 146.46, 133.39, 132.42, 131.57, 131.46, 128.59, 125.34, 125.21, 122.13, 111.32, 110.74, 90.25, 87.56, 83.79, 76.12, 52.65, 47.04, 39.45, 36.94; MS(FAB) m/z calcd for $C_{72}H_{65}N_3S_6$ = 1163, found = 1164 ($[M + H]^+$).

Synthesis of Biotinylated Tetraethylene Glycol Linker (*7*). To a solution of D-biotin (Sigma-Aldrich, 390 mg, 1.59 mmol) and HBTU (664 mg, 1.75 mmol) in DMF (6 mL), DIPEA (Lancaster, 0.6 mL) was added slowly and the milky reaction mixture turned to orange. Subsequently, linker **6** (347 mg, 1.59 mmol) in DMF (0.5 mL) was added and reaction mixture was stirred overnight under N_2 atmosphere at room temperature. The reaction mixture was extracted with CH_2Cl_2 (75 mL), washed with H_2O (25 mL) and NH_4Cl (25 mL), and then concentrated *in vacuo* to give an orange-colored oil. The crude mixture was purified by silica gel flash chromatography CH_2Cl_2-MeOH (10:1) to $CH_2Cl_2-MeOH-Et_3N$ (10:1:0.05) to yield **7** (0.536 g, 1.21 mmol, y = 76%): R_f = 0.50 ($CHCl_3-MeOH$ (10:1), spots were visualized by a phosphomolybdic acid stain); mp 91−93 °C; IR (thin film) 3392 (s), 2927, 2871, 2111, 1690 (s), 1648 (s), 1554, 1462, 1347, 1267, 1119, 938; ^1H NMR (400 MHz, $CDCl_3$) δ 6.90 (t, 1H, J = 5.4 Hz, amide N***H***), 6.82 (s, 1H, biotin ureido N***H***), 5.94 (s, 1H, biotin ureido N***H***), 4.48 (m, 1H, biotin $-SCH_2CHNH-CONH-$), 4.28 (m, 1H, biotin $-SCH(CH_2-)CHNHCONH-$), 3.58−3.68 (m, 10H, OEG $-OCH_2CH_2O-$), 3.55 (t, J = 5.1 Hz, 2H, OEG $-OCH_2CH_2NHCO-$), 3.41 (m, 2H, OEG $-OCH_2-CH_2NHCO-$), 3.38 (m, 2H, OEG $-OCH_2CH_2N_3$), 3.12 (m, 1H, biotin $-SCH(CH_2-)CHNH-$), 2.87 (dd, J = 12.9 Hz, 4.8 Hz, 1H, biotin $-SCH(H)CHNH-$), 2.73 (d, J = 12.8 Hz, 1H, biotin $-S CH(H)CHNH-$), 2.21 (t, J = 7.4 Hz, 2H, biotin $-CH_2CONH-$), 1.59−1.79 and 1.36−1.46 (m, 6H, biotin $-CH_2CH_2CH_2CH_2-CONH-$); ^{13}C NMR (100 MHz, $CDCl_3$) δ 173.63, 164.48, 70.76, 70.58, 70.18, 70.15, 70.11, 61.90, 60.37, 55.90, 50.78, 40.68, 39.25, 36.14, 28.44, 28.24, 25.82; HRMS(ESI) m/z calcd for $C_{18}H_{32}N_6O_5SNa$ = 467.2053, found = 467.2038 ($[M + Na]^+$).

Synthesis of Molecular Tip A. The biotinylated linker **7** (0.102 g, 0.23 mmol, 1.1 equiv) and tripod scaffold molecule **5** (0.250 g, 0.21 mmol, 1.0 equiv) were added to THF in the presence of *N*,*N*-diisopropyl ethylamine and the reaction mixture was degassed by freeze−pump−thaw. Subsequently, CuI was added and reaction mixture was stirred at 60 °C for 2 days. The reaction mixture was concentrated *in vacuo* to dryness and obtained crude mixture was dissolved in CH_2Cl_2 (60 mL) and washed with a mixture of NH_4OH-NH_4Cl (9:1, v/v, 20 mL) twice to remove any remaining copper. The organic layer was dried over Na_2SO_4 and concentrated *in vacuo* to give a yellowish solid. This solid was washed three times with CH_2Cl_2 (5 mL) to remove excess azide **7** to give a brownish, powdery solid **8** (0.294 g, 0.18 mmol, y = 85%): mp > 260 (dec); IR (KBr) 3414, 3079, 3040, 2922(s), 2853, 2205, 1700, 1603, 1521, 1466, 1399, 1353, 1286, 1217, 1180, 1167, 1138, 1012, 900, 817, 553; ^1H NMR (400 MHz, DMSO-d_6) δ 8.50 (s, 1H, triazole), 7.3−7.9 (overlapping, 4H, Ar***H***), 7.62 (d, 6H, J = 8.7 Hz, Ar***H***), 7.46 (d, 6H, J = 8.7 Hz, Ar***H***), 7.33 (d, 6H, J = 8.7 Hz, Ar***H***), 6.73 (d, 6H, J = 8.7 Hz, Ar***H*** *ortho* to amine), 6.7 (overlapping, 1H, amide N***H***), 6.38 (s, 1H, biotin ureido N***H***), 6.32 (s, 1H, biotin ureido N***H***), 4.56 (t, 2H, J = 4.4 Hz, triazole $-CH_2CH_2O-$), 4.26 (m, 1H, biotin $-SCH_2CHNH-CONH-$), 4.09 (m, 1H, biotin $-SCH(CH_2-)CHNHCONH-$), 3.95 (br t, 12H, $-NCH_2CH_2SS-$), 3.87 (t, J = 4.9 Hz, 2H, triazole $-CH_2CH_2O-$), 3.3−3.6 (m, 12H, OEG $-OCH_2-CH_2O-$), 3.14 (m, 1H, biotin $-SCH(CH_2-)CHNH-$), 3.08 (br t, 12H, $-NCH_2CH_2SS-$), 2.78 (dd, J = 12.3 Hz, 5.0 Hz, 1H, $-SCH(H)CHNH-$), 2.55 (d, J = 11.9 Hz, 1H, biotin $-SCH(H)CHNH-$), 2.12 (br s, 12H, adamantane), 2.03 (t, 2H, J = 7.0 Hz, biotin $-CH_2CONH-$), 1.35−1.63 (m, 6H, biotin $-CH_2CH_2CH_2CH_2CONH-$); ^{13}C NMR (100 MHz, DMSO-d_6) δ 172.07, 162.66, 149.34, 146.69, 133.70, 132.72, 130.77, 128.52, 125.75, 125.59, 124.99, 121.51, 120.79, 111.41, 108.74, 90.31, 87.27, 68.64−69.78, 61.00, 59.16, 57.51, 55.40, 52.03, 49.97, 49.56, 38.40, 36.21, 35.07, 28.17, 28.01, 25.24; MS(MALDI−TOF) m/z calcd for $C_{90}H_{97}N_9O_5S_7Na$ = 1630.6, found = 1630.6 ($[M + Na]^+$).

Immobilization of Molecular Tips on the AFM Tip. Gold-coated silicon nitride cantilevers (NPG, Veeco Instruments, Santa Barbara CA) were cleaned by irradiation of UV light (222 nm) for 30 min to remove any adsorbed organic materials. Immediately after irradiation, they were soaked overnight in 100 μM solution of molecular tip **A**, **B**, or **C** in DMSO (HPLC grade, Sigma-Aldrich) using a homemade Teflon-coated cantilever holder. Subsequently, they were washed with DMSO, EtOH, and H_2O exhaustively and attached to the AFM for force spectroscopy experiments.

AFM Force Spectroscopy Measurement and Analysis. All the force measurements were carried out with a Molecular Force Probe (MFP-1D AFM, Asylum Research, Santa Barbara, CA) using Igor Pro 4.09 software. The NeutrAvidin cross-linked agarose beads (immobilized NeutrAvidin Protein 29200, Pierce Biotechnology Inc., Rockford, IL) were placed on a glass slide in 20 mM HEPES buffer (pH 7.4). Force curve measurements were carried out with a scan rate of 0.12 Hz, tip velocity of 500 nm/s, distance of 2 μm, and loading rate of approximately 10^5 pN/s. Spring constants were calibrated by the thermal noise method before and after modification and were generally between 100−150 pN/nm. As a control experiment, force curve measurements were done (1) with cleaned gold-coated cantilever with no molecular tip, (2) with sepharose CL-6BC (cross-linked 6% agarose), and (3) in the presence of excess amount of biotin (0.22 mg/mL) in buffer. The rupture distance and force for each rupture peak in the retraction curve was recorded and subjected to histogram analysis.

Acknowledgment. We are grateful to Mr. Benjamin Rancatore, an undergraduate researcher in UCSB, for his technical help on synthesis of molecular tips. We thank Dr. Ken Nakazawa at the National Institute of Health Sciences of Japan and Dr. Thomas R. R. Pettus at UCSB for their advice and fruitful discussion. This work was supported in part by the Nano/Bio Interface Center of University of Pennsylvania through the National Science Foundation NSEC DMR-0425780 and by Japan Parmacopeia International Program.

Supporting Information Available: Text giving additional experimental details and data, structures of the compounds, schemes showing the syntheses, figures showing NMR, MS, and IR spectra and a histogram analysis, and a table giving the probability of ligand−receptor interaction observation. This material is available free of charge via the Internet at http://pubs.acs.org.